

Article

Surface and Underground Geomechanical Characterization of an Area Affected by Instability Phenomena in Zaruma Mining Zone (Ecuador)

Paúl Carrión-Mero ^{1,2,*} , Maribel Aguilar-Aguilar ^{1,*}, Fernando Morante-Carballo ^{1,3} ,
María José Domínguez-Cuesta ⁴ , Cristhian Sánchez-Padilla ⁵, Andrés Sánchez-Zambrano ⁶,
Josué Briones-Bitar ¹, Roberto Blanco-Torrens ⁷, Javier Córdova-Rizo ⁸ and Edgar Berrezueta ⁹ 



Citation: Carrión-Mero, P.; Aguilar-Aguilar, M.; Morante-Carballo, F.; Domínguez-Cuesta, M.J.; Sánchez-Padilla, C.; Sánchez-Zambrano, A.; Briones-Bitar, J.; Blanco-Torrens, R.; Córdova-Rizo, J.; Berrezueta, E. Surface and Underground Geomechanical Characterization of an Area Affected by Instability Phenomena in Zaruma Mining Zone (Ecuador). *Sustainability* **2021**, *13*, 3272. <https://doi.org/10.3390/su13063272>

Academic Editor: Stefano Morelli

Received: 9 February 2021

Accepted: 8 March 2021

Published: 16 March 2021

Publisher's Note: MDPI stays neutral with regard to jurisdictional claims in published maps and institutional affiliations.



Copyright: © 2021 by the authors. Licensee MDPI, Basel, Switzerland. This article is an open access article distributed under the terms and conditions of the Creative Commons Attribution (CC BY) license (<https://creativecommons.org/licenses/by/4.0/>).

- ¹ Centro de Investigaciones y Proyectos Aplicados a las Ciencias de la Tierra (CIPAT), Escuela Superior Politécnica del Litoral, ESPOL Polytechnic University, Campus Gustavo Galindo Km 30.5 Vía Perimetral, P.O. Box 09-01-5863 Guayaquil, Ecuador; fmorante@espol.edu.ec (F.M.-C.); briones@espol.edu.ec (J.B.-B.)
 - ² Facultad de Ingeniería en Ciencias de la Tierra, Escuela Superior Politécnica del Litoral, ESPOL Polytechnic University, Campus Gustavo Galindo Km 30.5 Vía Perimetral, P.O. Box 09-01-5863 Guayaquil, Ecuador
 - ³ Geo-Recursos y Aplicaciones GIGA, Facultad de Ciencias Naturales y Matemáticas, Escuela Superior Politécnica del Litoral, ESPOL Polytechnic University, Campus Gustavo Galindo Km 30.5 Vía Perimetral, P.O. Box 09-01-5863 Guayaquil, Ecuador
 - ⁴ Departamento de Geología, Universidad de Oviedo, Calle Jesús Arias de Velasco, s/n, 33005 Oviedo, Spain; dominguezmaria@uniovi.es
 - ⁵ Department of Informatics, Stuttgart University of Applied Sciences, 70174 Stuttgart, Germany; 92sacr1mpg@hft-stuttgart.de
 - ⁶ Independent Consultor, P.O. Box 09-01-5863 Guayaquil, Ecuador; anjosanc@espol.edu.ec
 - ⁷ Facultad de Geología y Minas, Instituto Superior Minero Metalúrgico (ISMM), 83310 Moa, Cuba; rblanco@espol.edu.ec
 - ⁸ Facultad de Ciencias Matemáticas y Físicas, Universidad de Guayaquil, Ciudadela Universitaria “Salvador Allende”, 090514 Guayaquil, Ecuador; francisco.cordovar@ug.edu.ec
 - ⁹ Departamento de Infraestructura Geocientífica y Servicios, Instituto Geológico y Minero de España (IGME), 33005 Oviedo, Spain; e.berrezueta@igme.es
- * Correspondence: pcarrion@espol.edu.ec (P.C.-M.); maesagui@espol.edu.ec (M.A.-A.); Tel.: +593-99-826-5290 (P.C.-M.); +593-98-286-3190 (M.A.-A.)

Abstract: In the last decade, in the mining district of Zaruma-Portovelo, there has been significant land subsidence related to uncontrolled mining activity. The purpose of this work was to carry out a surface and underground geomechanical characterization of a mining sector north of the city of Zaruma that allows the definition of potentially unstable areas susceptible to the mass movement. The methodology used consists of the following stages: (i) compilation of previous studies; (ii) surface and underground characterization of rocky material to establish its susceptibility to mass movement; (iii) interpretation of results; and (iv) proposal of action measures. Among the most relevant results, it stands out that 26.1% of the 23 stations characterized on the surface present conditions that vary from potentially unstable to unstable. In underground galleries, the studied mean values of the 17 stations indicate that the rock has a medium to good quality, representing a medium susceptibility to gallery destabilization. The results obtained for the surface areas (depths up to 50 m, where altered materials predominate) and the underground areas (depths > 50 m, where the alterations are specific) can be used to identify the areas with a more significant potential for instability. For both cases, it has been possible to define specific monitoring, control, and planning actions for sensitive areas.

Keywords: Zaruma; mining; geomechanical characterization; landslide susceptibility; land instability; subsidence

1. Introduction

Geological events related to land instability (mass movements, rock falls, and subsidence) are natural phenomena conditioned, fundamentally, by soil and rock properties,

topography, rainfall, and vegetation [1–6]. In general, instabilities have caused significant damage to civil infrastructure with significant economic losses [7–11]. However, the most notable thing is that these phenomena put people's lives at risk [5,12] and cause irreversible environmental damage [8,9,13].

According to a number of studies [12,14,15], human activity also has a notable influence on this geological phenomenon type, mainly due to the induced modifications in the land. A particular case of these activities is mining, which, when properly developed, favors the economy and develops the regions where a resource is exploited. In uncontrolled mines or without the due technical considerations, adverse effects can be caused in environmental aspects and ground instability [16–19]. Subsidence is a frequent geological problem in extractive activities of solid resources [9,13,20–31] and liquid resources [10,32,33]. If mining operations are developed in urban environments, it is necessary to carry out geological–geotechnical studies to establish this safety initiative. Thus, “urban geoscience” has been revealed as a new interdisciplinary field necessary in city planning and development to evaluate the geological environment and make possible the subsoil's strategic management [8].

Land susceptibility to instability and its geomechanical characterization have been addressed in various studies [10,13,21,23,26,28,32,34–44]. In these contributions, methods were developed to identify and to zone potential risk areas and, in a complementary way, to facilitate the implementation of preventive strategies that provide solutions to current instability problems [45].

The studied area corresponds to the north of Zaruma city (Ecuador). This locality is located in Southern Ecuador (Figure 1a), in the El Oro province, and it is part of the central gold-bearing districts [46–48]. This gold potential has allowed the development of intense and extensive mining activity through different types of exploitation. Thus, in the Zaruma environment, it is possible to identify both large legal mines and illegal mines (that are sometimes just a few dozen meters from the surface, without stabilization strategies). From the orographic point of view, the environment presents high slopes where mass movements linked to triggers such as heavy rainfalls, deforestation, seismic activity, civil works (e.g., roads), and mining are frequent. Since 2015, in addition to occasional landslides, there have been several subsidence events linked to the existence of illegal gold mining [16,38,49–51]. One of the most relevant subsidence events was the one that originated the collapse of the La Inmaculada School in the center of Zaruma in 2017 [49,51]. This event caused an increase in restrictions on mining activity below the urban area of Zaruma (Figure 1b) defined in the decree of the mining exclusion zone (EZ) (Ministerial Agreement No. 2017-002 [52]), issued by the relevant body of the Ecuadorian state (Ministry of Mining) [53]. Due to the city's subsidence reports, in 2017, the exclusion area had to be increased, covering the entire city. Furthermore, to prevent illegal mining from weakening the area, the decree was modified again, prohibiting mining activity in approximately 2.15 km² around Zaruma city. The study area encompasses part of the last mining exclusion zone (Figure 1b). Zaruma was selected as the case study due to its importance as a gold deposit in Ecuador and its particular geologic, geomorphologic, climatic, and orographic conditions. The specific study area was chosen to consider the possibility of accessing underground galleries in current exploitation (outside the exclusion zone) and without exploitation (within the exclusion area) belonging to the BIRA S.A. mining company.

The aim of this study was to carry out a surface and underground geological–geomechanical characterization of an area of 0.7 km² in the north of Zaruma. The plan was to: (i) define areas susceptible to subsidence based on the geomechanical characteristics of the rocks; (ii) identify areas of high susceptibility where mining activity must optimize its exploitation procedure to guarantee stability underground and on the surface; and (iii) propose measures to be taken regarding mining activities in the underground and land use planning on the surface.

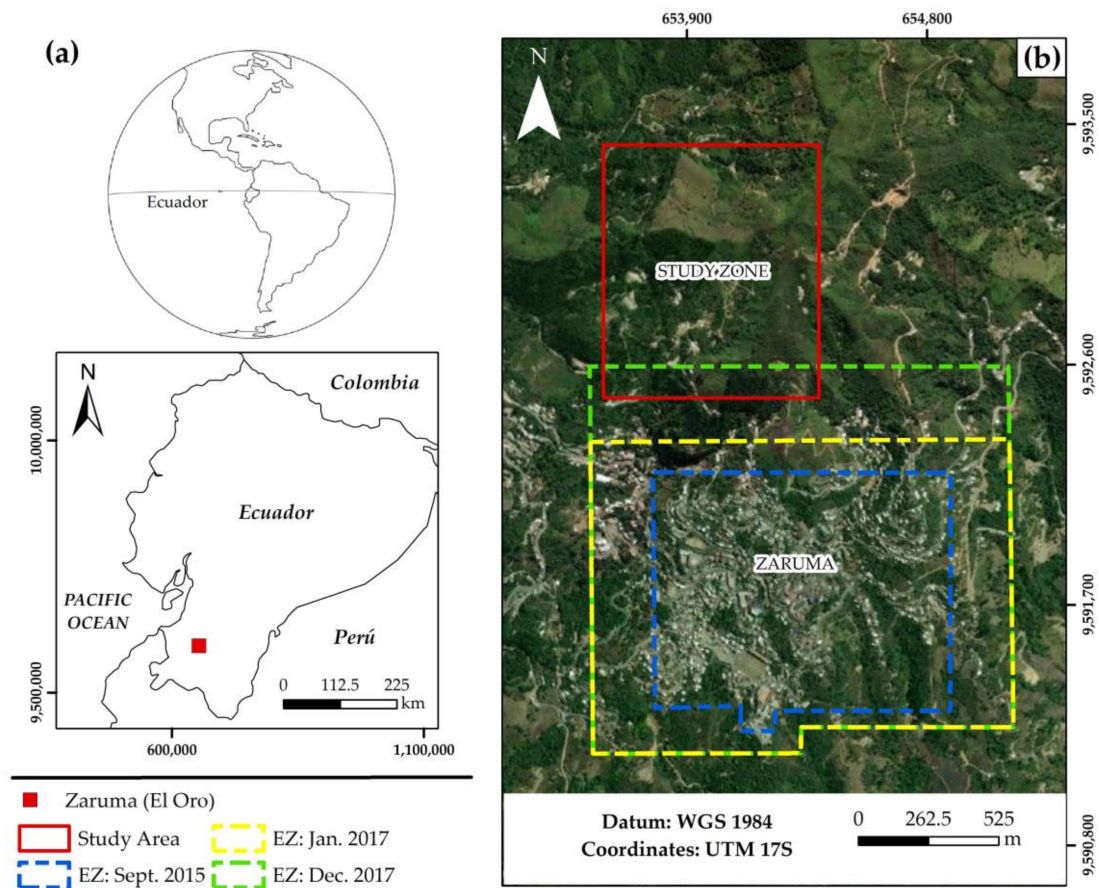


Figure 1. (a) Zaruma (El Oro, Ecuador) location; (b) location of the study area in the North of Zaruma. EZ: exclusion zone. Satellite image source [54].

2. Study Area

The morphology of Zaruma is characterized by steep slopes, rounded mountain ranges, and heights between 1150 and 2800 m a.s.l. The predominant geoforms of the area corresponds to heterogeneous slopes, with medium to strong slopes [49].

The lithology within the study area (Figure 2a,b) consists of metamorphic, igneous, and sedimentary rocks ranging from the Precambrian–Paleozoic to the Quaternary age [55]. The basement rocks are metamorphic rocks (Triassic). Above them, massive andesitic lavas are unconformably intruded by small plutons of diorite to granodiorite composition (Lower Cretaceous). Felsic volcanic lavas, pyroclastics, and rhyolitic flows (Tertiary–Miocene) unconformably cap all of these units. Finally, Quaternary alluvial and colluvial deposits can be recognized along the Amarillo and Calera rivers [56]. According to Van Thournout et al., 1996, the mineralization in this area was originated by collapse and post-collapse rhyolitic activity. The Zaruma area (Figure 2b) is part of the epithermal vein system (Zaruma-Portovelo). This epithermal vein system is the result of hydrothermal processes close to a Miocene volcano that produced an andesitic to dacitic sequence. The identified ore and gangue mineral assemblages are typical for intermediate sulfidation epithermal gold vein deposits ($\text{Au} \pm \text{Ag} \pm \text{Cu}$) associated with Early Miocene continental arc magmatism [55,57]. The gold exploitation in Zaruma is trough underground mining used in epithermal deposits of in the vein system. The galleries are horizontal excavations into the side of hills or mountains, and levels are excavated horizontally off the decline to access the ore body. The distance between exploitation levels is approximately 30 m. In general, the deposit is extracted using the chambers and pillars method or a cut and fill method in which empty spaces are filled as the mineral is extracted.

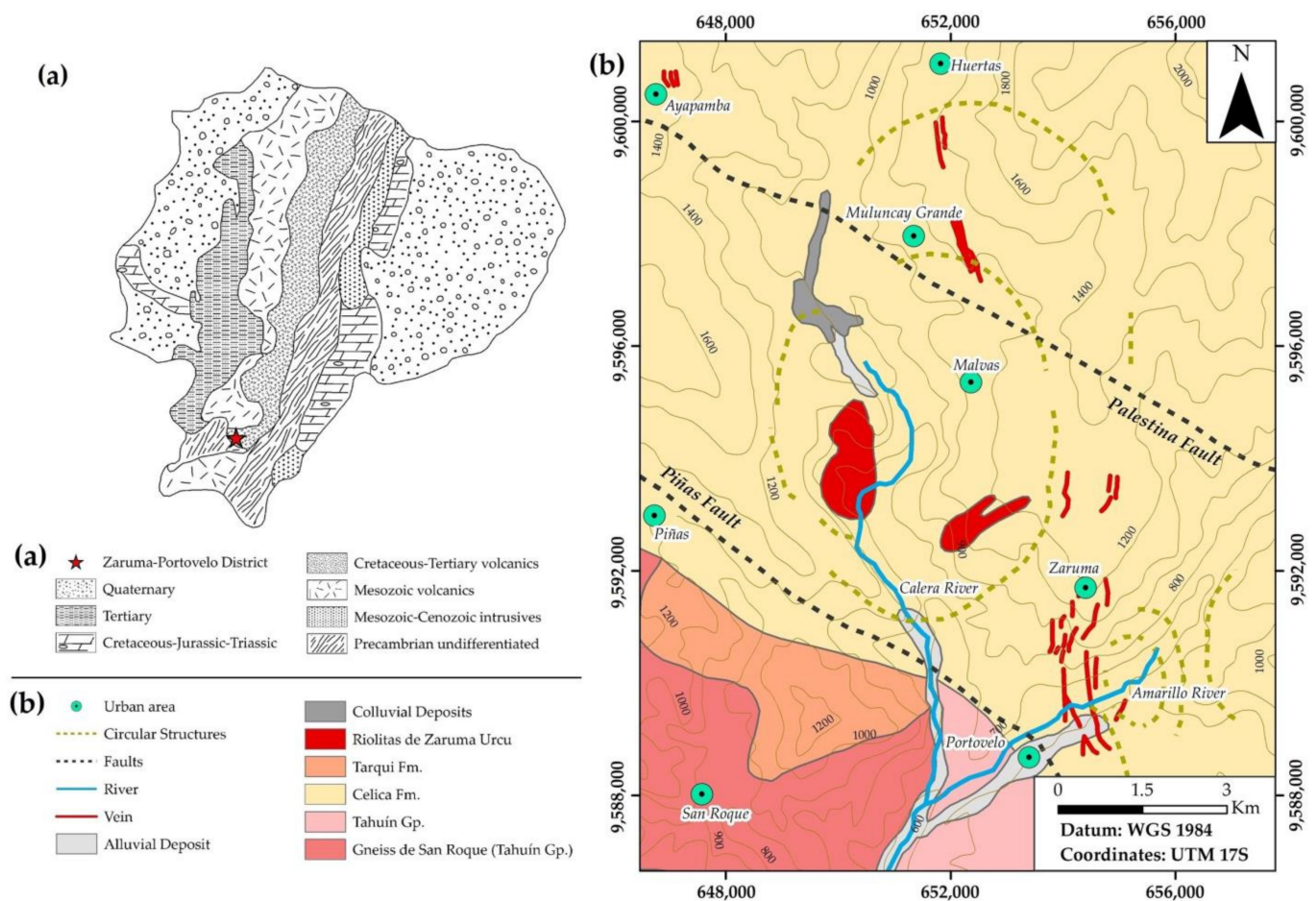


Figure 2. (a) Location of the Zaruma-Portovelo deposit on the simplified geological map of Ecuador. (b) Zaruma-Portovelo geological map, with prominent veins, structures, and geological formations. Adapted from [58]; Adapted with permission from ref. [59]. Copyright 2009 Universidad de Buenos Aires.

Geomorphologically, the most prominent feature is the rugged relief corresponding to the Southern Andes of Ecuador, characterized by the marked fluvial incision and the absence of stratovolcanoes [60]. Zaruma's climate is classified as subtropical, dry from May to November, and humid from December to April. In the study area, as occurs in sub-tropical environments, high rainfall during six months of the year originates essential chemical processes that generate deep weathering profiles. Regarding the vegetation cover, the area initially corresponded to a premontane forest. Currently, many of these areas are used for agriculture and livestock. The alteration and transformation of the rock into saprolite and residual soils represent an essential determining factor when evaluating land stability. Zaruma city occupies an area of approximately 1 km² and 10,000 inhabitants. The main economic activities are mining, agriculture, livestock, and tourism.

3. Materials and Methods

The procedure followed in this study is divided into three main different phases (Figure 3): (i) information processing and systematization, (ii) surface and underground survey, and (iii) interpretation and evaluation of results.

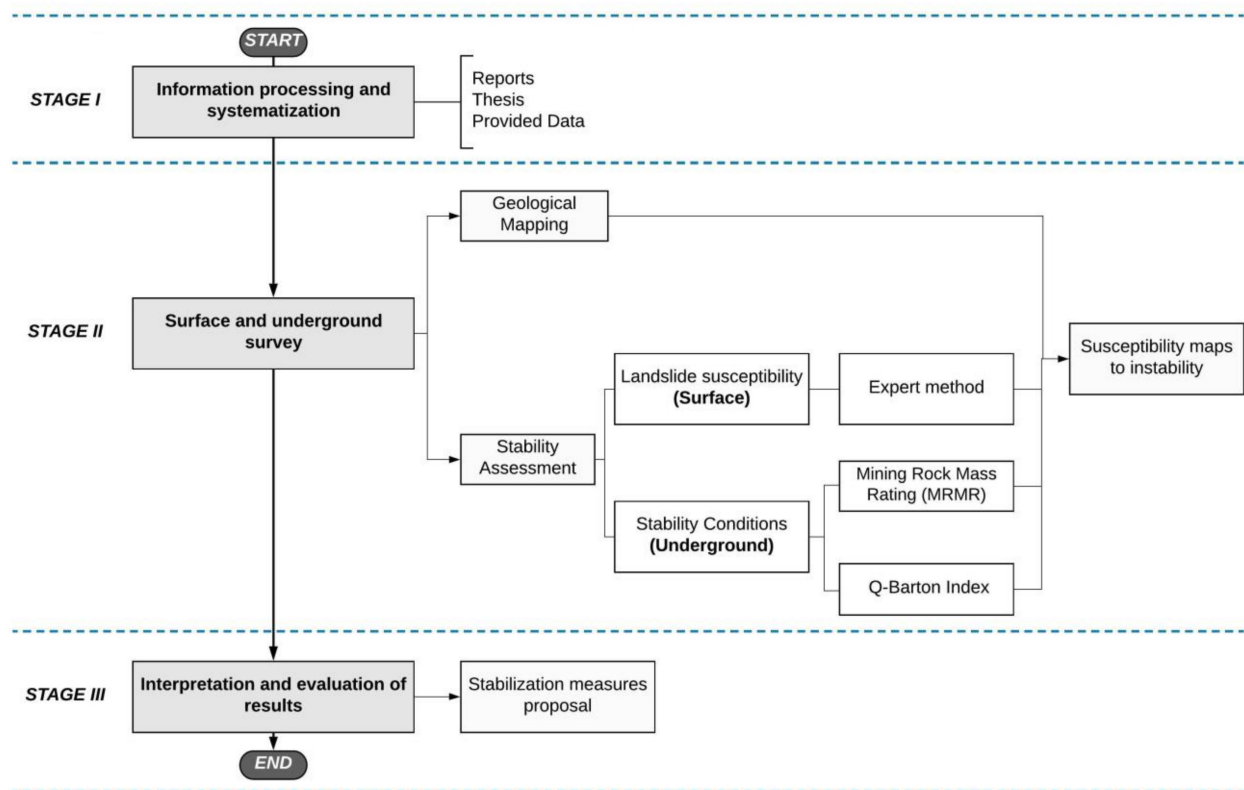


Figure 3. Methodology scheme used for the assessment of instability phenomena in the north of the Zaruma mining zone.

3.1. Stage I: Information Processing and Systematization

The study began with the collection and review of previous studies carried out in the area [61–64], specifically, with a collection of data from boreholes, topography, and general geological maps provided, in most cases, by BIRA S.A. mining company. The fieldwork campaign was designed in order to complete the data needed to determine the area's state of stability at the surface and underground level. The characterization methods are detailed in Section 3.2.

3.2. Stage II: Surface and Underground Survey

This stage included the geological and geomechanical characterization of rocks on the surface (outcrops) [65] and underground (galleries) [34,35]. During the first sampling campaign, 23 stations were selected for geologic and geomechanical characterization through a study of outcrops. In the second sampling campaign, 17 stations were taken for geologic and geomechanical characterization through a study of galleries. The number of stations studied was limited due to budget constraints, access permits, terrain, and gallery conditions. This aim of this phase of the work was to obtain susceptibility maps of instability at the surface and underground level.

3.2.1. Surface Characterization

The surface study addressed the prominent outcrop characterization and 23 stations in the study area (Figure 4). The number of stations and location depend on the favorable terrain conditions (existing outcrops and accessibility). At first, the primary lithology to be characterized in each sampling station was defined from the general lithology identified from the outcropping study. Next, through specific theoretical–practical methodology application used in landslides by various authors [65–69], the rocks' geomechanical characteristics were defined (Table 1) by assigning evaluations made following expert criteria. The selected parameters were lithology, geological structure, morphometry, discontinuity, water, vegetable cover, seismic activity, and weathering rank, which were evaluated from 0

to 4 (Table S1) based on the conditions observed in the field. This method allows the susceptibility level to landslide (Table 2) to be defined. The susceptibility level is a qualitative value (I to V), and it is related to the susceptibility coefficient (SC) estimated [70,71]. Thus, the grade or susceptibility level are: I for $SC < 5$; II for $5 < SC < 10$; III for $10 < SC < 15$; IV for $15 < SC < 20$; and V for $SC > 20$. As a result, susceptibility maps of instability were prepared from the geomechanical evaluations obtained by using the geostatistical kriging tool that allows the values to be interpolated.

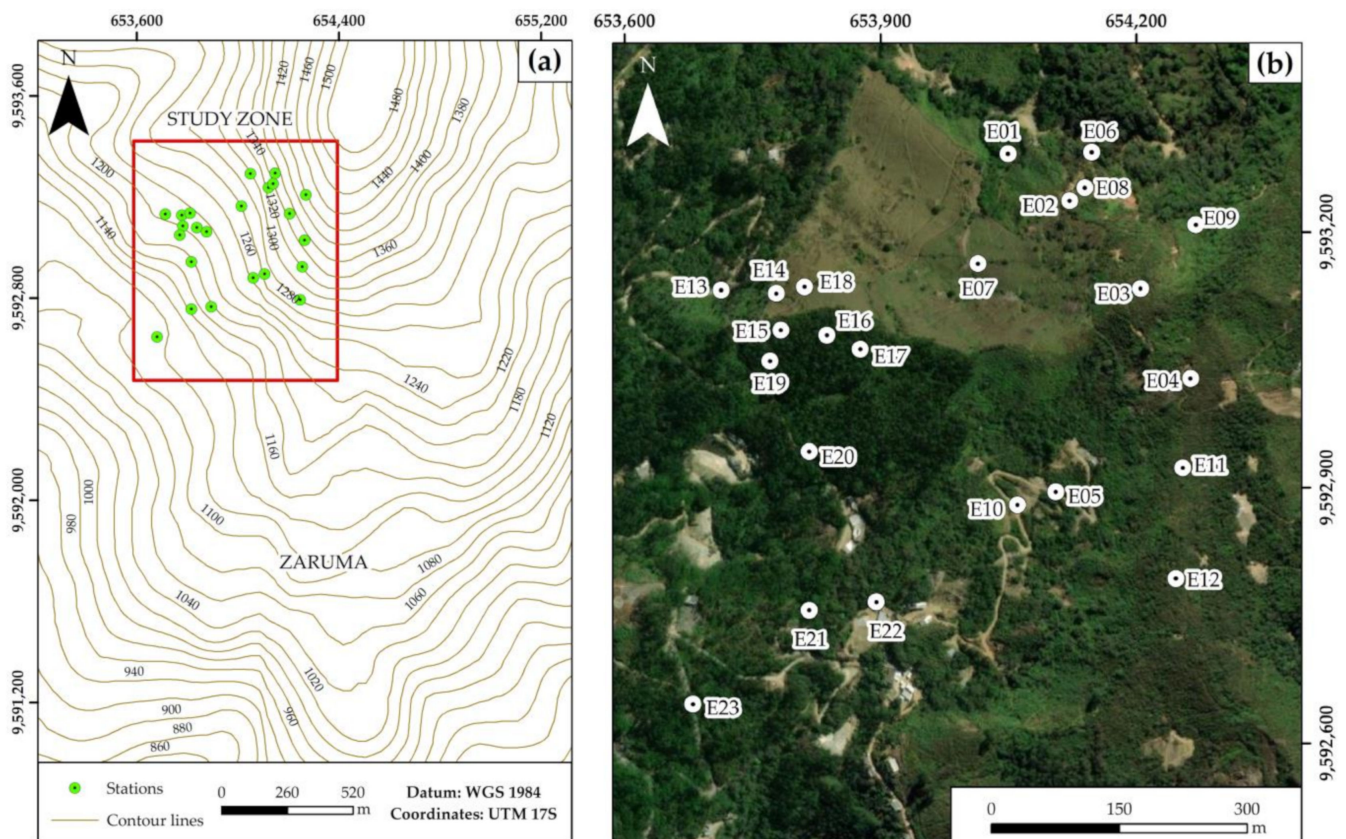


Figure 4. (a) Position of the study area and location of the stations defined for surface characterization in this work. (b) Detail of the surface stations [54].

Table 1. Main parameters and weights assigned to rock massifs in the susceptibility coefficient estimation [65–69].

Parameters	Weight
Lithology (L)	0 to 4
Geological structure (Gs)	0 to 4
Morphometry (M)	0 to 4
Discontinuity (D)	0 to 4
Water (W)	0 to 3
Vegetable cover (Vc)	0 to 3
Seismic (S)	0 to 4
Weathering Rank (Wr)	0 to 4
SC: (L + Gs + M + D + W + Vc + S + Wr)	0 to 30

Table 2. Landslide susceptibility classification for rock massifs [65–69].

Susceptibility Level	Susceptibility Coefficient (SC)	Remark
I	Very low: $SC < 5.0$	Stable conditions.
II	Low: $5 < SC < 10$	Stable conditions. Monitoring is required.
III	Medium: $10 < SC < 15$	Predominantly stable conditions. Systematic monitoring is required.
IV	High: $15 < SC < 20$	Potentially unstable conditions.
V	Very high: $SC > 20$	Unstable conditions.

3.2.2. Underground Characterization

The underground characterization was carried out in mining galleries at depths greater than 50 m, with the permission of Bienes Raices S.A. mining company (BIRA S.A.). Specifically, this stage focused on the geological and geomechanical analysis of the rock samples from the 17 sampling stations (Figure 5) located in the mining galleries. The location of the stations was selected based on the accessibility conditions and galleries that are outside the mining exclusion zone. As in the surface characterization phase, the stage was to identify the most representative rock types in each of the defined stations and their main characteristics (physical and chemical alterations). Next, an instability evaluation of the galleries was carried out using two evaluation methodologies applied for the 17 underground stations: (i) Q-Barton Index [34] and (ii) Mining Rock Mass Rating [35], which allow the comparison and validation of the rock quality results. The Mining Rock Mass Rating (MRMR) method was applied in order to validate Q-Barton method. Both methods allow zoning of the rock quality and its susceptibility level, based on the valuation interpolation using the kriging tool.

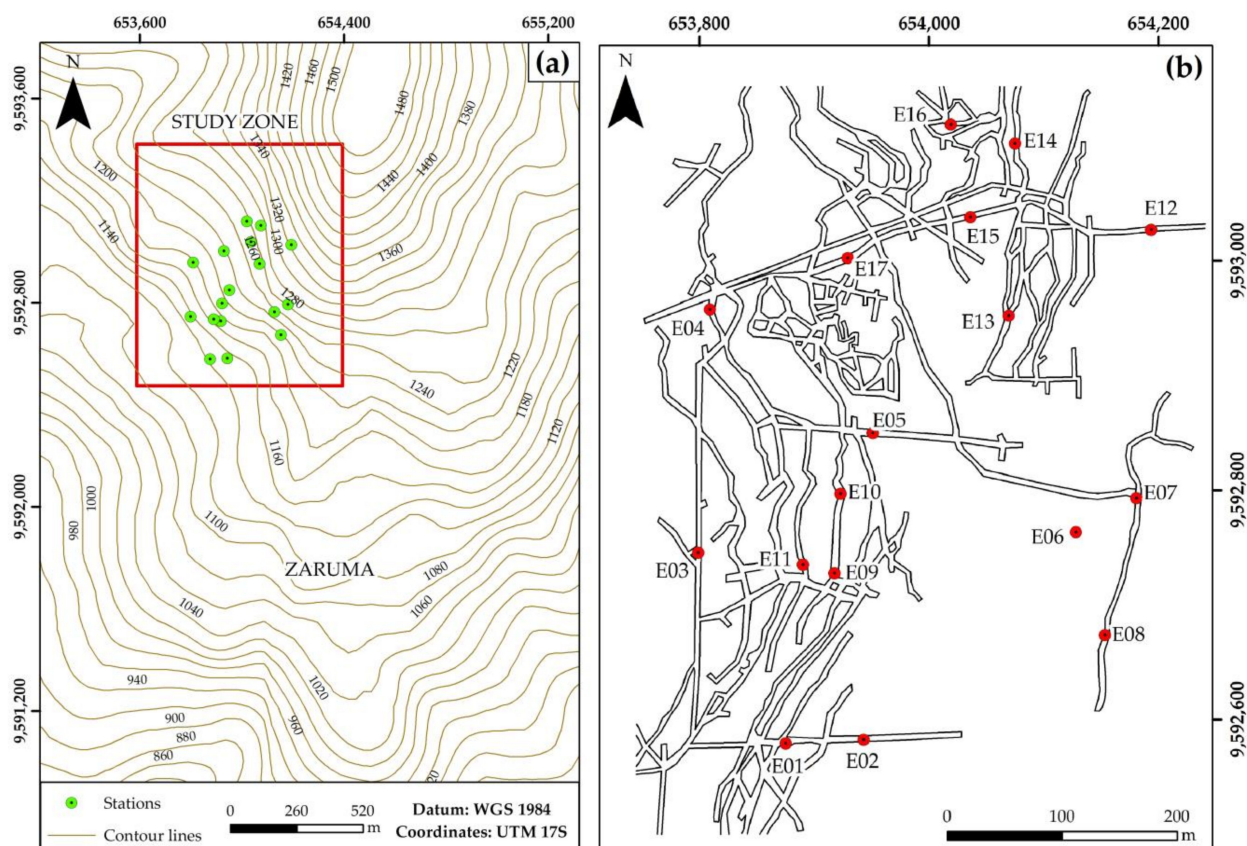


Figure 5. (a) Location of defined stations for underground characterization (in galleries) in this work. (b) Detail of the stations' position on the underground work plan provided by BIRA S.A mining company. Levels between 1214 and 1318 m.

Q-Barton Index

The method proposed by Barton, Lien, and Lunde [34], evaluates the rocks' geomechanical behavior (Equation (1)) and establishes a qualitative classification of their quality (Table 3) through the use of six parameters: rock quality designation (RQD) [72,73], joint roughness number (Jr), joint set number (Jn), joint alteration number (Ja), joint water reduction factor (Jw), and stress reduction factor (SFR) [34] (Table S2). These parameters were obtained from field surveys in existing tunnels, which allow the issuance of criteria for the sizing of new tunnels. In order to be able to compare the surface and underground characterization, a parameter defined in the surface rocks (susceptibility level, Table 2) is also included in Table 3. The susceptibility level is a qualitative value (I to V) included in the analysis and inspired by previous work [74–76], the authors of which proposed a direct relationship between Q-Barton RQD and susceptibility. In addition, due to the lack of coincidence in the number of classes between Q-Barton (9) and the levels of susceptibility (5), the value of susceptibility III (3/5) was assigned to the fair value (5/9).

$$Q = (RQD/Jn)*(Jr/Ja)*(Jw/SRF) \quad (1)$$

Table 3. Rock quality according to the Q Index [34]. * Based on susceptibility level values defined in Table 2.

Q-Barton	Rock Massif Quality	Susceptibility Level *
0.001–0.01	Exceptionally poor	V
0.01–0.1	Extremely poor	V
0.1–1	Very poor	IV
1–4	Poor	IV
4–10	Fair	III
10–40	Good	II
40–100	Very good	II
100–400	Extremely good	I
400–1000	Exceptionally good	I

Mining Rock Mass Rating (MRMR)

The MRMR method proposed by Reference [35] is used to perform rock mass valuation including aspects related to mining and combines several parameters for the mass valuation (RMR [77]), considering such criteria as mining-induced stresses (Cs), blasting effects (Cb), weathering (Cw), and joint orientation (Co) (Table S3). Using the weighted sum of different parameters, and with Equation (2), the MRMR value was obtained.

$$MRMR = RMR*Cw*Co*Cs*Cb, \quad (2)$$

From the MRMR values obtained, the massif's behavior can be qualitatively characterized (Table 4).

Table 4. Rock quality according to MRMR [35]. * Susceptibility level values defined from Table 2.

MRMR	Rock Massif Quality	Susceptibility Level *
0–20	Very poor	V
20–40	Poor	IV
40–60	Fair	III
60–80	Good	II
80–100	Very good	I

A parameter defined for the surface rocks was added to the qualitative qualification of the rock quality (susceptibility level, Tables 2 and 4) in order to enable comparisons between the surface and underground characterization. The susceptibility level is a qualitative value

(I to V) included in the analysis and inspired by previous work [78,79], the authors of which proposed a direct relationship between MRMR and susceptibility. In this case, 5 levels of susceptibility were assigned to 5 levels of MRMR analysis.

3.3. Stage III: Interpretation of Results and Stabilization Proposals

Based on the susceptibility level to the mass movement (surface analysis) and rockfall (underground analysis), the obtained results (susceptibility level maps) were evaluated to establish recommendations for stabilization strategies in the most susceptible sectors.

4. Results

4.1. Surface Characterization

4.1.1. Geological Characterization

The data collected in surface outcrops made it possible to determine the primary lithology. Thus, (i) altered rhyolitic tuff to the NE of the study area, (ii) porphyritic andesite and siliceous breccia to the S, and (iii) intrusive diorite to the NW were identified. The predominant structural trend in the area is NS (Figure 6a). The lithological reconstruction (Figure 6b) using the data of previously carried out perforations in the study area shows that there are potent layers of andesite and porphyritic andesite at the base of this regular column without relevant alteration (thicknesses greater than 45 m). Overlaying these layers, an intercalation of altered tuff/tuff/tuff agglomerate (approximately 45 m) is identified. Over this intercalation, a layer of white fractured breccia (5 m) is identified, and finally, in the upper 5 m, weathered rock (saprolite) of brown color appears.

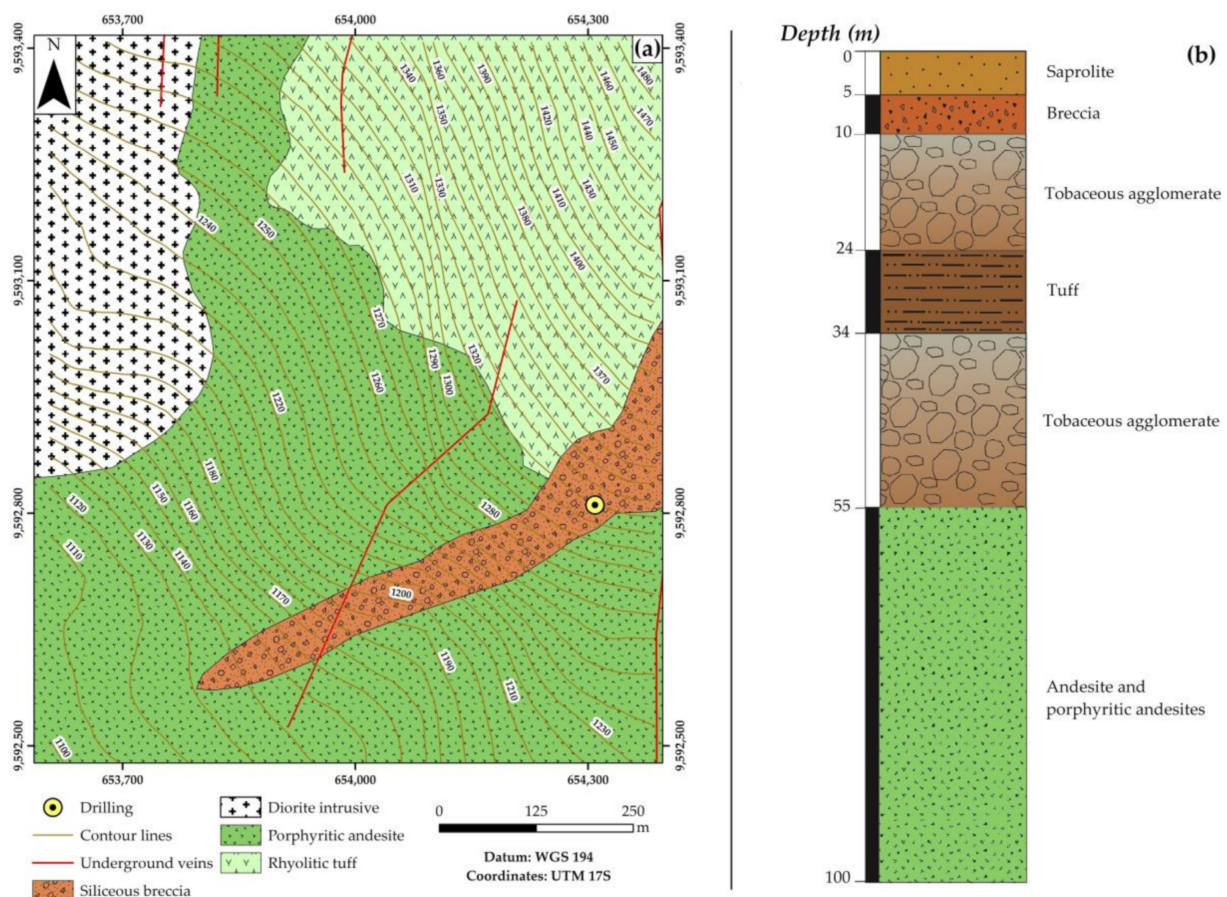


Figure 6. (a) Geological map of the study area. (b) Stratigraphic column of the substrate rocks in the study area obtained from a survey provided by BIRA S.A. mining company. Drilling takes place in the yellow dot.

4.1.2. Lithological Sampling and Characterization

The detailed reconnaissance of the 23 stations allowed the detailed geological characterization through the identification, sampling, and analysis of rock samples (defined most often as rhyolitic tuff and porphyritic andesite), although with characteristics of saprolite and weathered rock. Table 5 presents the lithological characterization and the main description of these surface samples.

Table 5. Lithological characterization of surface samples.

Station	Lithology (Original Rock)	Main Description
1	Rhyolitic tuff	Saprolite
2	Rhyolitic tuff	Rock somewhat weathered and with some weathering degree
3	Rhyolitic tuff	Saprolite
4	Rhyolitic tuff	Rock somewhat weathered and with some weathering degree
5	Porphyritic andesite	Rock somewhat weathered and with some weathering degree
6,9	Rhyolitic tuff	Saprolite
7	Rhyolitic tuff	Rock somewhat weathered and with some weathering degree
8	Rhyolitic tuff	Rock somewhat weathered and with some weathering degree
10	Porphyritic andesite	Saprolite
11	Rhyolitic tuff	Rock somewhat weathered and with some weathering degree
12	Siliceous breccia	Rock somewhat weathered and with some weathering degree
13,14	Diorite intrusive	Saprolite
15	Diorite intrusive	Rock somewhat weathered and with some weathering degree
16	Porphyritic andesite	Saprolite
17,18	Porphyritic andesite	Saprolite
19	Diorite intrusive	Rock somewhat weathered and with some weathering degree
20	Porphyritic andesite	Saprolite
21,22,23	Porphyritic andesite	Saprolite

The results obtained from evaluating susceptibility level in rocky massifs and altered rock indicate that: 26.1% of the stations present conditions that vary from potentially unstable to unstable. The remaining 73.9% are stable, and they need monitoring (Table 6 and Figure 7b). Figure 7a shows a zoning map of the studied area based on the obtained susceptibility conditions.

Table 6. Global results of the susceptibility level (Table 1) and landslide susceptibility categories (Table 2) estimated for 23 stations.

Station	Susceptibility Coefficient	Susceptibility Level	Observations
1	16.5	IV	Potentially unstable conditions.
2	12.5	III	Predominantly stable conditions. Systematic monitoring is required.
3	16	IV	Potentially unstable conditions.
4	16.5	IV	Potentially unstable conditions.
5	9	II	Stable conditions. Monitoring is required.
6	16	IV	Potentially unstable conditions.
7	10.5	III	Predominantly stable conditions.
8	10.5	III	Systematic monitoring is required.
9	12.5	IV	Potentially unstable conditions.
10	10.5	III	Predominantly stable conditions. Systematic monitoring is required.

Table 6. Cont.

Station	Susceptibility Coefficient	Susceptibility Level	Observations
11	6.5	II	Stable conditions. Monitoring is required.
12	5.5		
13	9.5	III	Predominantly stable conditions. Systematic monitoring is required.
14	10		
15	13		
16	9.5		
17	9		
18	8	II	Stable conditions. Monitoring is required.
19	8		
20	20.5	V	Unstable conditions.
21	14	III	Predominantly stable conditions. Systematic monitoring is required.
22	7.5	II	Stable conditions. Monitoring is required.
23	7.5		

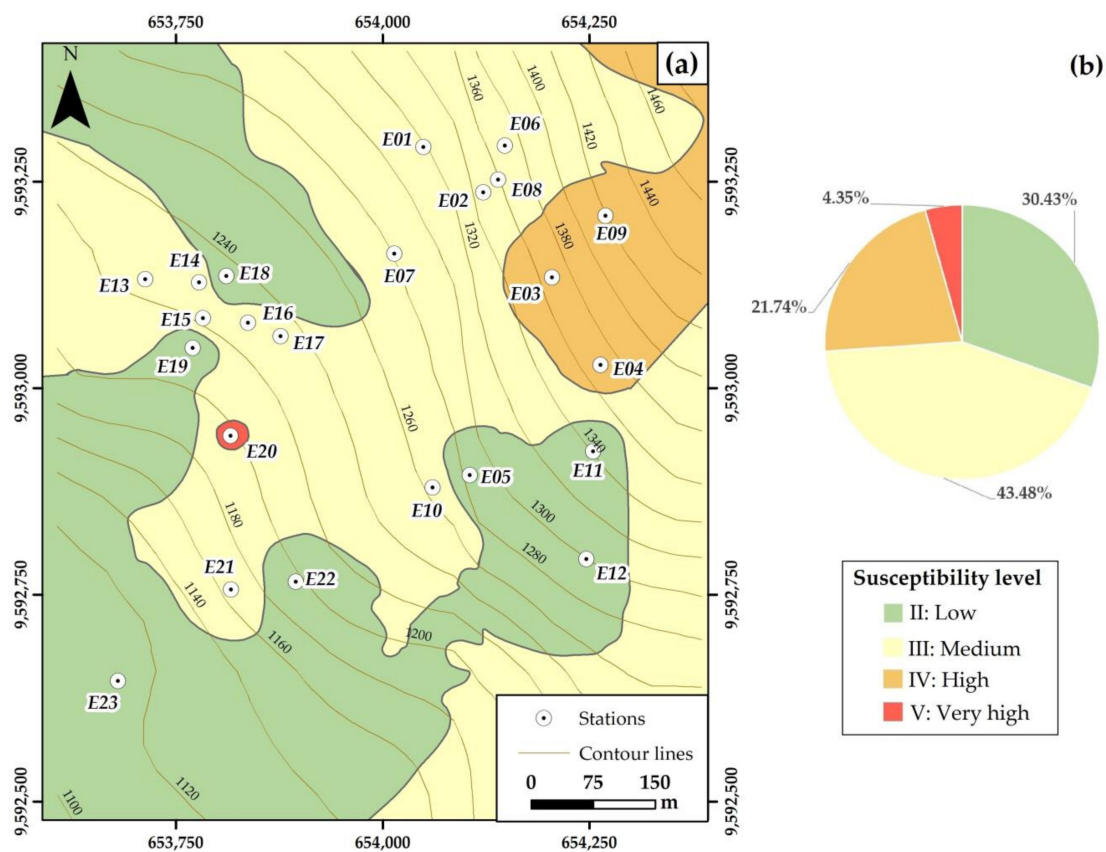


Figure 7. (a) Susceptibility level map of instabilities built based on the data obtained on the surface and (b) classification of the results obtained for landslide susceptibility, considering the 23 surface stations.

4.2. Underground Characterization

4.2.1. Geological Characterization

The lithologies identified in the 17 underground stations evaluated are described in Table 7. The primary lithologies identified, in addition to the ore materials (quartz veins of approximately 2 m), are andesite, diorite, microdiorite, and rhyolitic tuff. It was also possible to define the degree of fracturing and alteration of these rocks (Table 7) in this study.

Table 7. Lithological characterization of underground samples.

Stations	Lithology (L)	General Description
1,6	Andesite	Slightly weathered and fractured andesite, with a greenish-grey hue. The rocky massif is fractured into blocks, with rough surfaces and little evidence of deterioration.
2	Microdiorite	Slightly deteriorated and fractured microdiorite, with rough surfaces without deterioration. Greenish-grey rock.
3,4,8	Andesite	Andesite without evidence of deterioration, of a greenish-grey hue. The rocky massif is moderately fractured, with fresh and rough surfaces.
5,7	Microdiorite	Microdiorite without deterioration, with a greenish-grey hue, presents few fractures with very rough surfaces and without deterioration.
9	Andesite with dioritic dike	Slightly deteriorated rock with a light green hue. The rocky massif has block fracturing and rough fracture surfaces with ferrous spots.
10,13,16	Porphyritic andesite	Slightly deteriorated rock with a greenish-grey hue, showing areas of mylonites. The rocky massif presents fracturing in blocks with rough surfaces and high deterioration.
11	Diorite	Slightly deteriorated rock with a greenish-gray hue, the rocky massif presents intense fracturing with rough surfaces without deterioration.
12,17	Rhyolitic tuff	Porous rocks slightly altered and deteriorated, with a pink hue.
14,15	Dioritic intrusive	Rock without deterioration, fractured with rough surfaces, of a greenish-gray hue.

4.2.2. Geomechanical Characterization

The evaluation of the underground rocky massif quality, through the analysis of the different mine stations using the Q-Barton method, indicates that 41.18% of the evaluated stations correspond to the rocky massif of good to very good quality (detachment susceptibility of II in Table 8), while 35.29% correspond to fair quality rock (detachment susceptibility III in Table 8), and finally 23.53% represent rock of poor quality (detachment susceptibility in Table 9) (Figure 8b). Figure 8a shows a map zoning the studied area based on the rock mass quality obtained, based on the Q-Barton method.

Table 8. Results obtained for underground stations by the Q-Barton method.

Station	Jn	Jr	Ja	Jw	RQD (%)	SRF	Q-Barton Index	Qualitative Rating	Susceptibility Level
1	4	2.00	2.00	1.00	94.72	1.00	23.68	Good	II
2	4	2.00	2.00	0.66	96.02	5.00	3.17	Poor	IV
3	5	2.00	0.80	1.00	90.21	1.00	45.11	Very Good	II
4	5	1.50	0.90	0.66	90.60	1.50	13.29	Good	II
5	9	2.00	0.90	0.50	82.66	1.50	7.20	Fair	III
6	3	1.50	2.00	0.50	96.31	1.00	12.04	Good	II
7	3	2.00	2.00	0.50	94.37	1.20	13.11	Good	II
8	9	1.50	2.00	0.33	90.21	1.00	2.48	Poor	IV
9	3	1.50	4.00	0.50	83.98	1.00	5.25	Fair	III
10	6	1.00	5.00	0.33	93.24	1.00	1.03	Poor	IV
11	3	2.00	1.50	0.66	94.72	1.00	27.79	Good	II
12	3	1.50	2.00	1.00	77.25	1.50	12.84	Good	II
13	5	1.50	2.00	0.50	81.39	1.00	6.08	Fair	III
14	3	1.50	2.00	0.33	88.63	1.00	7.34	Fair	III
15	7	1.50	2.00	0.50	79.07	1.00	4.23	Fair	III
16	9	1.50	2.00	0.33	87.81	1.00	2.42	Poor	IV
17	3	1.00	3.50	0.66	83.92	1.00	5.28	Fair	III

Note: Jn—joint set number; Jr—joint roughness number; Ja—joint alteration number; Jw—joint water reduction factor; RQD—rock quality designation; SRF—stress reduction factor.

Table 9. Results obtained by MRMR method for underground stations.

Station	RMR	Cw	Co	Cs	Cb	MRMR	Qualitative Rating	Susceptibility Level
1	68.80	0.94	0.90	1.20	1	69.87	Good	II
2	63.10	0.94	0.90	1.20	1	65.28	Good	II
3	66.50	1.00	0.90	1.20	1	71.92	Good	II
4	61.00	1.00	0.80	1.20	1	58.66	Fair	III
5	47.40	1.00	0.80	1.20	1	45.52	Fair	III
6	65.40	0.94	0.90	1.20	1	66.42	Good	II
7	65.20	1.00	0.90	1.20	1	70.44	Good	II
8	50.90	0.94	0.90	1.20	1	51.68	Fair	III
9	58.50	0.94	0.80	1.20	1	52.88	Fair	III
10	60.80	0.94	0.80	1.20	1	54.90	Fair	III
11	68.10	1.00	0.90	1.20	1	73.57	Good	II
12	52.30	0.94	0.90	1.20	1	53.12	Fair	III
13	51.90	0.94	0.9	1.2	1	52.70	Fair	III
14	51.90	0.94	0.9	1.2	1	52.76	Fair	III
15	47.70	0.94	0.9	1.2	1	48.53	Fair	III
16	46.50	0.94	0.9	1.2	1	47.28	Fair	III
17	50.00	0.76	0.9	1.2	1	41.10	Fair	III

Note: RMR, rock mass rating; Cw, weathering; Co, joint orientation; Cs, mining-induced stresses; Cb, blasting effects.

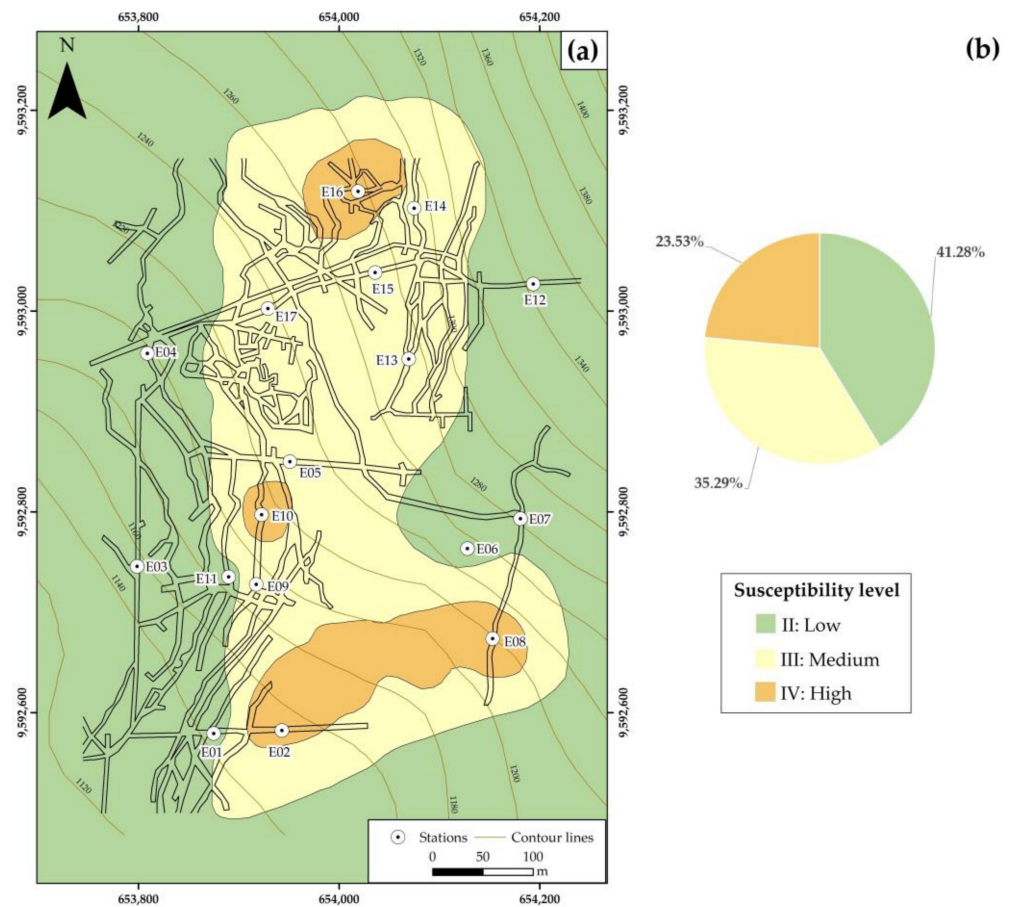


Figure 8. (a) Zoning of the underground exploitation area according to the geomechanical evaluation applying the Q-Barton method in the tunnel stations and (b) classification of the results obtained from the underground stations' evaluation using the Q-Barton method.

On the other hand, 64.71% of the rock mass evaluated with the MRMR method presents fair rock quality (detachment susceptibility III in Table 9), while 35.29% corresponds to good rock quality (detachment susceptibility II in Table 9) (Figure 9b). Figure 9a shows a map zoning the studied area based on the rock mass quality obtained by the MRMR method.

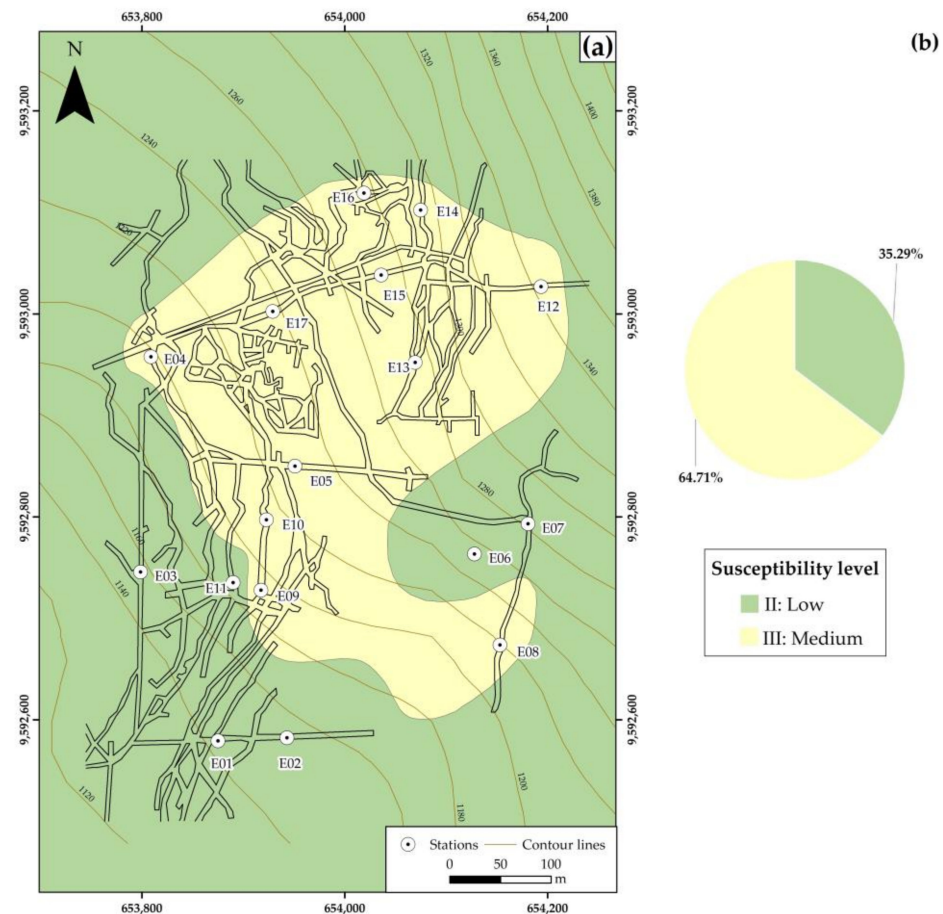


Figure 9. (a) Zoning of the underground exploitation area according to the geomechanical evaluation applying the MRMR method and (b) classification of the results obtained from evaluating the underground stations' using the MRMR method.

5. Interpretation of Results and Discussion

The geological characterization carried out, both in the outcrops and surface stations and in the underground stations in the study area, revealed two geological scenarios: first of all, an area denominated superficial (up to about 50 m deep, Figure 6b) where the materials present an evident weathering as a consequence, mainly, of an intense chemical alteration. This alteration does not prevent the original rock's recognition, although its physical properties are profoundly modified (Table 5), compromising its strength and stability. Just below this zone appears the so-called underground zone (depths greater than 50 m). In this deeper zone, the rocks do not present significant alterations, except in some specific areas, due to the hydrothermal activity that produced the deposit's mineralization. It should be noted that the depth of 50 m mentioned corresponds to the maximum depth at which, in this study, the presence of generally altered rock was detected. In some areas, it was found that the altered rock layer has small thicknesses.

In the surface stability analysis, the applied land stability evaluation methodology [65–69] made it possible to define a susceptibility map of instability in the study area (Figure 7). This contribution is considered very relevant because it allows characterization of the low land stability and, in particular, its low potential to support underground mining operations.

In the case of underground materials, the two methods used (Q-Barton Index and MRMR) could be used to obtain comparable results to zone the areas susceptible to instabilities (Figures 8 and 9). Thus, the Q-Barton method presents a land categorization with lower values (23.53% of the stations rock of poor quality; 35.29% fair quality; 41.18% good-very good quality) than the MRMR method (64.71% of the stations rock of regular quality; 35.29% good). Underground stations classified with the worst qualities in both methods are characterized by presenting conjugate fracture systems and water presence. As shown in Figures 8 and 9, the most detailed results are provided by the Q-Barton method.

Given the stability conditions defined in the zoning maps, it is advisable to propose actions that guarantee the safety of the area, preventing instabilities from affecting the population and infrastructures. These proposals are summarized below:

- In surface areas with high susceptibility to instability (susceptibility levels IV and V), it is recommended to improve the surface drainage system, prepare a reforestation plan, and restrict urban development. Illegal mining activities must be stopped to avoid endangering the population.
- In underground areas susceptible to instabilities (susceptibility level above III), it is recommended to improve the water drainage systems in all galleries, use better methods and materials to support gallery ceilings, and use the filling of sterile chambers in addition to the support pillars.
- In the closest areas to the urban area, it is recommended to extend the study with additional surface and underground geomechanical stations to obtain a metric scale susceptibility model.

6. Conclusions

The application of the evaluation processes used allowed the zoning of areas with a potential risk of land instability in the mining environment of Zaruma. The information collected on the surface (outcrops and sampling stations) and in underground galleries (sampling stations) made it possible to verify that there is an area up to 50 m thick in which the altered rock predominates. It does not present guarantees of stability to carry out extractive works.

The susceptibility maps of instability phenomena (subsidence and landslides) generated in this work are adequate spatial planning tools. Thus, they can be used as a basis for the proposal of measures to limit the subsidence within the city's urban area and safeguard its population's lives.

Supplementary Materials: The following are available online at <https://www.mdpi.com/2071-1050/13/6/3272/s1>, Table S1: Parameters used for the susceptibility assessment, Table S2: Descriptions and ratings for the Jr, Jn, Ja, and Jw parameters, Table S3: Descriptions and ratings for the C.D., Cw, Co, Cs, and Cb parameters.

Author Contributions: Conceptualization, P.C.-M., F.M.-C., M.A.-A.; methodology, P.C.-M., F.M.-C., M.A.-A., J.B.-B., M.J.D.-C. and E.B.; validation, P.C.-M., F.M.-C., M.J.D.-C. and E.B.; investigation, C.S.-P., A.S.-Z., F.M.-C. and J.C.-R.; data curation, M.A.-A.; writing—original draft preparation, C.S.-P., A.S.-Z., R.B.-T., P.C.-M. and F.M.-C.; writing—review and editing, M.A.-A., P.C.-M., F.M.-C., M.J.D.-C., E.B. and J.B.-B.; visualization, M.A.-A., C.S.-P., A.S.-Z.; supervision, P.C.-M., F.M.-C., R.B.-T., M.J.D.-C. and E.B.; project administration, P.C.-M., F.M.-C. and J.B.-B. All authors have read and agreed to the published version of the manuscript.

Funding: This research was funded by ESPOL Polytechnic University research project "Propuesta de Geoparque Ruta del Oro y su incidencia en el desarrollo territorial, CIPAT-02-2018".

Institutional Review Board Statement: Not applicable.

Informed Consent Statement: Not applicable.

Data Availability Statement: The data presented in this study are available in article and supplementary material.

Acknowledgments: This work has been made possible thanks to supporting and access permits from BIRA Bienes Raíces S.A. Mining Company to carry out field visits accompanied by technicians in underground galleries. This work is based on previous initiatives sponsored by the Red Minería XXI (CYTED: 407310RT0402, IGME). The authors would like to thank three anonymous reviewers for their constructive comments and the editorial office for the editorial handling.

Conflicts of Interest: The authors declare no conflict of interest.

References

1. Van Dao, D.; Jaafari, A.; Bayat, M.; Mafi-Gholami, D.; Qi, C.; Moayedi, H.; Van Phong, T.; Ly, H.-B.; Le, T.-T.; Trinh, P.T.; et al. A spatially explicit deep learning neural network model for the prediction of landslide susceptibility. *Catena* **2020**, *188*, 104451. [CrossRef]
2. Corominas, J.; Moya, J. A review of assessing landslide frequency for hazard zoning purposes. *Eng. Geol.* **2008**, *102*, 193–213. [CrossRef]
3. Van Westen, C.J. The Modelling of Landslide Hazards Using GIS. *Surv. Geophys.* **2000**, *21*, 241–255. [CrossRef]
4. Akbar, F.; Asupyani, H.; Azizi, H.A. Geological Hazards Interpretation Using Remote Sensing Method in Cimahi District, Kuningan Region, West Java. *IOP Conf. Ser. Earth Environ. Sci.* **2020**, *412*, 012022. [CrossRef]
5. Yang, W.; Ding, R.; Zhou, Z.; Li, L.; Shi, S.; Wang, M.; Zhang, Q.; Geng, Y. Improved Attribute Interval Evaluation Theory for Risk Assessment of Geological Disasters in Underground Engineering and Its Application. *Geotech. Geol. Eng.* **2020**, *38*, 2465–2477. [CrossRef]
6. Sousa, R.L.; Einstein, H.H. Risk analysis during tunnel construction using Bayesian Networks: Porto Metro case study. *Tunn. Undergr. Space Technol.* **2012**, *27*, 86–100. [CrossRef]
7. Scavia, C.; Barbero, M.; Castelli, M.; Marchelli, M.; Peila, D.; Torsello, G.; Vallero, G. Evaluating Rockfall Risk: Some Critical Aspects. *Geosciences* **2020**, *10*, 98. [CrossRef]
8. De Rienzo, F.; Oreste, P.; Pelizza, S. Subsurface geological-geotechnical modelling to sustain underground civil planning. *Eng. Geol.* **2008**, *96*, 187–204. [CrossRef]
9. Bell, F.G.; Donnelly, L.J.; Genske, D.D.; Ojeda, J. Unusual cases of mining subsidence from Great Britain, Germany and Colombia. *Environ. Earth Sci.* **2004**, *47*, 620–631. [CrossRef]
10. Ng, A.H.-M.; Ge, L.; Li, X.; Abidin, H.Z.; Andreas, H.; Zhang, K. Mapping land subsidence in Jakarta, Indonesia using persistent scatterer interferometry (PSI) technique with ALOS PALSAR. *Int. J. Appl. Earth Obs. Geoinf.* **2012**, *18*, 232–242. [CrossRef]
11. Primanita, A. Jakarta Areas Muara Baru, Cengkareng Sinking Fast. *Jakarta Globe* 2010. Available online: <http://www.thejakartaglobe.com/archive/jakarta-areas-muara-baru-cengkareng-sinking-fast/> (accessed on 20 December 2020).
12. Cappadonia, C.; Di Maggio, C.; Agate, M.; Agnesi, V. Geomorphology of the urban area of Palermo (Italy). *J. Maps* **2020**, *16*, 274–284. [CrossRef]
13. Du, Z.; Ge, L.; Ng, A.H.-M.; Li, X. Investigation on mining subsidence over Appin–West Cliff Colliery using time-series SAR interferometry. *Int. J. Remote Sens.* **2017**, *39*, 1528–1547. [CrossRef]
14. Sánchez, J.R.B. Paul J. Crutzen: A Pioneer on Atmospheric Chemistry and Climate Change in the Anthropocene. *Ambix* **2016**, *63*, 359–360. [CrossRef]
15. Cooper, A.H.; Brown, T.J.; Price, S.J.; Ford, J.R.; Waters, C.N. Humans are the most significant global geomorphological driving force of the 21st century. *Anthr. Rev.* **2018**, *5*, 222–229. [CrossRef]
16. Carrión-Mero, P.; Loo-Oporto, O.; Andrade-Ríos, H.; Herrera-Franco, G.; Morante-Carballo, F.; Jaya-Montalvo, M.; Aguilar-Aguilar, M.; Torres-Peña, K.; Berrezueta, E. Quantitative and Qualitative Assessment of the “El Sexmo” Tourist Gold Mine (Zaruma, Ecuador) as A Geosite and Mining Site. *Resources* **2020**, *9*, 28. [CrossRef]
17. Mert, Y. Contribution to sustainable development: Re-development of post-mining brownfields. *J. Clean. Prod.* **2019**, *240*, 118212. [CrossRef]
18. Mancini, L.; Sala, S. Social impact assessment in the mining sector: Review and comparison of indicators frameworks. *Resour. Policy* **2018**, *57*, 98–111. [CrossRef]
19. Cao, X. Regulating mine land reclamation in developing countries: The case of China. *Land Use Policy* **2007**, *24*, 472–483. [CrossRef]
20. Gutierrez, F.; Ortí, F.; Gutiérrez, M.; Pérez-González, A.; Benito, G.; Prieto, J.G.; Valsero, J.J.D. The stratigraphical record and activity of evaporite dissolution subsidence in Spain. *Carbonates Evaporites* **2001**, *16*, 46–70. [CrossRef]
21. Mancini, F.; Stecchi, F.; Gabbianelli, G. GIS-based assessment of risk due to salt mining activities at Tuzla (Bosnia and Herzegovina). *Eng. Geol.* **2009**, *109*, 170–182. [CrossRef]
22. Mancini, F.; Stecchi, F.; Zanni, M.; Gabbianelli, G. Monitoring ground subsidence induced by salt mining in the city of Tuzla (Bosnia and Herzegovina). *Environ. Earth Sci.* **2008**, *58*, 381–389. [CrossRef]
23. Stecchi, F.; Antonellini, M.; Gabbianelli, G. Curvature analysis as a tool for subsidence-related risk zones identification in the city of Tuzla (BiH). *Geomorphology* **2009**, *107*, 316–325. [CrossRef]
24. Crane, W. *Subsidence and Ground Movement in the Copper and Iron Mines of the Upper Peninsula, Michigan*; US Government Printing Office: Washington, DC, USA, 1929.
25. Marschalko, M.; Třeslín, L. Impact of underground mining to slope deformation genesis at Doubrava Ujala. *Acta Montan. Slovaca* **2009**, *14*, 232–240.

26. Palchik, V. Prediction of hollows in abandoned underground workings at shallow depth. *Geotech. Geol. Eng.* **2000**, *18*, 39–51. [[CrossRef](#)]
27. Bauer, R.A.; Trent, B.A.; Dumontelle, P.B. *Mine Subsidence in Illinois: Facts for Homeowners*; Illinois State Geological Survey, Prairie Research Institute: Champaign, IL, USA, 1993.
28. Perski, Z.; Jura, D. Identification and measurement of mining subsidence with SAR interferometry: Potentials and limitations. In Proceedings of the 11th FIG Symposium on Deformation Measurements, Santorini, Greece, 25–28 May 2003; pp. 1–7.
29. Doyle, J. Notes on the salt mine of Duncrue. *Trans. Geol. Soc. Dublin* **1853**, *5*, 232–236.
30. Donnelly, L.J. Nevado del Ruiz Volcano, Galeras Volcano and the Manizales Volcanological & Seismological Observatory, Colombia, South America. *Br. Geol. Surv.* **1997**, *47*, 620–631. [[CrossRef](#)]
31. Antonio-Carpio, R.G.; Pérez-Flores, M.A.; Camargo-Guzmán, D.; Alanís-Alcantar, A. Use of resistivity measurements to detect urban caves in Mexico City and to assess the related hazard. *Nat. Hazards Earth Syst. Sci.* **2004**, *4*, 541–547. [[CrossRef](#)]
32. Perissin, D.; Wang, T. Time-Series InSAR Applications over Urban Areas in China. *IEEE J. Sel. Top. Appl. Earth Obs. Remote Sens.* **2011**, *4*, 92–100. [[CrossRef](#)]
33. Abidin, H.Z.; Andreas, H.; Gumilar, I.; Sidiq, T.P.; Gamal, M. Environmental Impacts of Land Subsidence in Urban Areas of Indonesia. In Proceedings of the FIG Working Week 2015: From the Wisdom of the Ages to the Challenges of Modern World, Sofia, Bulgaria, 17–21 May 2015; pp. 17–21.
34. Barton, N.; Lien, R.; Lunde, J. Engineering classification of rock masses for the design of tunnel support. *Rock Mech. Rock Eng.* **1974**, *6*, 189–236. [[CrossRef](#)]
35. Laubscher, D.H. Class distinction in rock masses. *Coal. Gold Base Min.* **1975**, *23*, 37–50.
36. Zarroca, M.; Linares, R.; Velásquez-López, P.C.; Roqué, C.; Rodriguez, R.F. Application of electrical resistivity imaging (ERI) to a tailings dam project for artisanal and small-scale gold mining in Zaruma-Portovelo, Ecuador. *J. Appl. Geophys.* **2015**, *113*, 103–113. [[CrossRef](#)]
37. Vidal Montes, R.; Martínez-Graña, A.M.; Martínez Catalán, J.R.; Ayarza Arribas, P.; Sánchez San Román, F.J. Vulnerability to groundwater contamination, SW salamanca, Spain. *J. Maps* **2016**, *12*, 147–155. [[CrossRef](#)]
38. Martínez-Graña, A.M.; Goy, J.L.; Cimarra, C. 2D to 3D geologic mapping transformation using virtual globes and flight simulators and their applications in the analysis of geodiversity in natural areas. *Environ. Earth Sci.* **2014**, *73*, 8023–8034. [[CrossRef](#)]
39. Roccati, A.; Paliaga, G.; Luino, F.; Faccini, F.; Turconi, L. GIS-Based Landslide Susceptibility Mapping for Land Use Planning and Risk Assessment. *Land* **2021**, *10*, 162. [[CrossRef](#)]
40. Sestras, P.; Bilaşco, Ş.; Roşca, S.; Naş, S.; Bondrea, M.; Gâlău, R.; Vereş, I.; Sălăgean, T.; Spalević, V.; Cîmpeanu, S. Landslides Susceptibility Assessment Based on GIS Statistical Bivariate Analysis in the Hills Surrounding a Metropolitan Area. *Sustainability* **2019**, *11*, 1362. [[CrossRef](#)]
41. Marsala, V.; Galli, A.; Paglia, G.; Miccadei, E. Landslide Susceptibility Assessment of Mauritius Island (Indian Ocean). *Geosciences* **2019**, *9*, 493. [[CrossRef](#)]
42. Erdogan, H.; Duzgun, H.; Selcuk-Kestel, A. Quantitative hazard assessment for Zonguldak Coal Basin underground mines. *Int. J. Min. Sci. Technol.* **2019**, *29*, 453–467. [[CrossRef](#)]
43. dos Santos, T.B.; Lana, M.S.; Pereira, T.M.; Canbulat, I. Quantitative hazard assessment system (Has-Q) for open pit mine slopes. *Int. J. Min. Sci. Technol.* **2019**, *29*, 419–427. [[CrossRef](#)]
44. Bhattacharya, A.; Arora, M.K.; Sharma, M.L. Usefulness of synthetic aperture radar (SAR) interferometry for digital elevation model (DEM) generation and estimation of land surface displacement in Jharia coal field area. *Geocarto Int.* **2012**, *27*, 57–77. [[CrossRef](#)]
45. Morante Carballo, F.; Carrión Mero, P.; Ángel Chávez, M.; Aguilar Aguilar, M.; Briones Bitar, J. Design of the stabilization solutions in the general patrimonial cemetery of Guayaquil, Ecuador. In Proceedings of the 17th LACCEI International for Multi-Conference for Engineering, Education, and Technology: “Industry, Innovation, and Infrastructure for Sustainable Cities Communities”, Montego Bay, Jamaica, 24–26 July 2019.
46. Lane, K. Unlucky strike: Gold and labor in Zaruma, Ecuador, 1699–1820. *Colon. Lat. Am. Rev.* **2004**, *13*, 65–84. [[CrossRef](#)]
47. Velásquez-López, P.C.; Veiga, M.M.; Hall, K. Mercury balance in amalgamation in artisanal and small-scale gold mining: Identifying strategies for reducing environmental pollution in Portovelo-Zaruma, Ecuador. *J. Clean. Prod.* **2010**, *18*, 226–232. [[CrossRef](#)]
48. Carrión Mero, P.; Blanco Torrens, R.; Borja Bernal, C.; Aguilar Aguilar, M.; Morante Carballo, F.; Briones Bitar, J. Geomechanical characterization and analysis of the effects of rock massif in Zaruma City, Ecuador. In Proceedings of the 17th LACCEI International for Multi-Conference for Engineering, Education, and Technology: “Industry, Innovation, and Infrastructure for Sustainable Cities Communities”, Montego Bay, Jamaica, 24–26 July 2019.
49. Jácome, M.C.; Martínez-Graña, A.M.; Valdés, V. Detection of Terrain Deformations Using InSAR Techniques in Relation to Results on Terrain Subsidence (Ciudad de Zaruma, Ecuador). *Remote Sens.* **2020**, *12*, 1598. [[CrossRef](#)]
50. Vangsnes, G.F. The meanings of mining: A perspective on the regulation of artisanal and small-scale gold mining in southern Ecuador. *Extr. Ind. Soc.* **2018**, *5*, 317–326. [[CrossRef](#)]
51. Ammirati, L.; Mondillo, N.; Rodas, R.A.; Sellers, C.; Di Martire, D. Monitoring Land Surface Deformation Associated with Gold Artisanal Mining in the Zaruma City (Ecuador). *Remote Sens.* **2020**, *12*, 2135. [[CrossRef](#)]

52. Agencia de Regulación y Control Minero. Ministerio de Minería Amplía Zona de Exclusión de Zaruma. Available online: www.controlminero.gob.ec/ministerio-de-mineria-amplia-zona-de-exclusion-de-zaruma/#:~:text=El%20Ministerio%20de%20Mi-ner%C3%ADa%20firm%C3%B3,El%20Oro%2C%20a%20173%20hect%C3%A1reas (accessed on 20 December 2020).
53. Franco, G.H.; Mero, P.C.; Carballo, F.M.; Narváez, G.H.; Bitar, J.B.; Torrens, R.B. Strategies for the development of the value of the mining-industrial heritage of the Zaruma-Portovelo, Ecuador, in the context of a geopark project. *Int. J. Energy Prod. Manag.* **2020**, *5*, 48–59. [CrossRef]
54. Esri World Imagery. Available online: http://goto.arcgisonline.com/maps/World_Imagery (accessed on 20 December 2020).
55. Van Thournout, F.; Salemink, J.; Valenzuela, G.; Merlyn, M.; Boven, A.; Muchez, P. Portovelo: A volcanic-hosted epithermal vein-system in Ecuador, South America. *Miner. Depos.* **1996**, *31*, 269–276. [CrossRef]
56. La Misión Británica y la Dirección General de Geología y Minas. *Hoja Geológica Zaruma 38 CT-NVI-E Escala 1:100,000*; Instituto de Investigación Geológico y Energético, Ministerio de Recursos Naturales y Energéticos, Dirección General de Geología y Minas: Quito, Ecuador, 1980.
57. Chiaradia, M.; Fontboté, L.; Beate, B. Cenozoic continental arc magmatism and associated mineralization in Ecuador. *Miner. Depos.* **2004**, *39*, 204–222. [CrossRef]
58. Berrezueta, E.; Ordóñez-Casado, B.; Bonilla, W.; Banda, R.; Castroviejo, R.; Carrión, P.; Puglla, S. Ore Petrography Using Optical Image Analysis: Application to Zaruma-Portovelo Deposit (Ecuador). *Geosciences* **2016**, *6*, 30. [CrossRef]
59. Bonilla, W. Metalogenia del Distrito Minero Zaruma-Portovelo, República del Ecuador. Ph.D. Thesis, Universidad de Buenos Aires, Buenos Aires, Argentina, 2009.
60. Sauer, W. *Geología del Ecuador*; Editorial Talleres Gráficos del Ministerio de Educación: Quito, Ecuador, 1965.
61. Sánchez Padilla, C.V.; Sánchez Zambrano, A.J. *Evaluación de Amenazas Geodinámicas en el Entorno de la Actividad Minera en la Concesión Minera Palacios (Tesis de Grado)*; Escuela Superior Politécnica del Litoral: Guayaquil, Ecuador, 2019.
62. Blanco, R. Estudios de la Zona de Exclusión Minera en los Cantones Zaruma-Portovelo: Caso concesiones mineras Esperanza II y Palacios. In *Informe Geotécnico*; CIPAT-ESPOLTECH E.P.: Guayaquil, Ecuador, 2018.
63. Secretaría de Gestión de Riesgos (SGR) Proyecto. *Perforaciones Geotécnicas en el Área de Interés del Casco Urbano de la Ciudad de Zaruma, Provincia de El Oro*; Secretaría de Gestión de Riesgos (SGR) Proyecto: Quito, Ecuador, 2018.
64. Morante, F. Estudios de la Zona de Exclusión Minera en los Cantones Zaruma-Portovelo: Caso Concesiones Mineras La Esperanza II y Palacios. In *Informe Geológico*; CIPAT-ESPOLTECH E.P.: Guayaquil, Ecuador, 2018.
65. Blanco, R. *Estudios y Propuestas de Estabilización del Cerro Las Cabras*; CIPAT-ESPOL: Guayaquil, Ecuador, 2015.
66. Nicholson, D.T.; Hencher, S. Assessing the potential for deterioration of engineered rock slopes. In *Proceedings of the Engineering Geology and the Environment*, Athens, Greece, 23–27 June 1997; Volume 1, pp. 911–917.
67. Anbalagan, R. Terrain evaluation and landslide hazard zonation for environmental regeneration and land use planning in mountainous terrain. In *Proceedings of the International Symposium on Landslides*, Rotterdam, The Netherlands, 10–14 February 1992; Volume 6, pp. 861–869.
68. Brand, E.W.; Phillipson, H.B. Sampling and testing of residual soils. In *A Review of International Practice*; Hong Kong Scorpion Press: Hong Kong, China, 2015.
69. Suarez, J. *Deslizamientos y Estabilidad de Taludes en Zonas Tropicales*; Instituto de Investigaciones sobre Erosión y Deslizamientos: Bucaramanga, Colombia, 1998.
70. Morgenstern, N.R.; Price, V.E. The Analysis of the Stability of General Slip Surfaces. *Géotechnique* **1965**, *15*, 79–93. [CrossRef]
71. Morante, F.; Aguilar, M.; Ramírez, G.; Blanco, R.; Carrión, P.; Briones, J.; Berrezueta, E. Evaluation of Slope Stability Considering the Preservation of the General Patrimonial Cemetery of Guayaquil, Ecuador. *Geosciences* **2019**, *9*, 103. [CrossRef]
72. Deere, D.U.; Deere, D.W. *Rock Quality Designation (RQD) after Twenty Years*; Geotechnical Laboratory, US Army Engineer Waterways Experiment Station: Vicksburg, MS, USA, 1988.
73. Priest, S.; Hudson, J. Discontinuity spacings in rock. *Int. J. Rock Mech. Min. Sci. Géoméch. Abstr.* **1976**, *13*, 135–148. [CrossRef]
74. Luo, Y.; Qiu, B. Identifying Root Causes for Subsidence over Abandoned Coal Mine—A Case Study. In *Proceedings of the 47th U.S. Rock Mechanics/Geomechanics Symposium*, San Francisco, CA, USA, 23–26 June 2013; p. 12.
75. Cuervas-Mon, J.; Jordá-Bordehore, L.; Nazareno, J.A.; Escobar, K.F. Evaluation of the stability of small diameter mining excavations using geomechanical classifications and empirical analysis: The case of the San Juan mine, Ecuador. *Trab. Geol.* **2015**, *35*, 19–28. [CrossRef]
76. Jordá-Bordehore, L.; Jordá-Bordehore, R.; Valsero, J.J.D.; Romero-Crespo, P.L. Evaluación de la estabilidad de las labores y pilar corona en las minas abandonadas de S'Argentera (Ibiza, España) combinando clasificaciones geomecánicas, métodos empíricos y análisis numérico-enfocado a su posible aprovechamiento turístico. *Boletín Geológico Min.* **2017**, *128*, 3–24. [CrossRef]
77. Bieniawski, Z.T. *Engineering Rock Mass Classifications: A Complete Manual for Engineers and Geologists in Mining, Civil, and Petroleum Engineering*; John Wiley & Sons: Hoboken, NJ, USA, 1989.
78. Lee, S.; Park, I.; Choi, J.-K. Spatial Prediction of Ground Subsidence Susceptibility Using an Artificial Neural Network. *Environ. Manag.* **2012**, *49*, 347–358. [CrossRef] [PubMed]
79. Laboratorio Oficial Madariaga-LOM. *Guía Sobre Control Geotécnico en Minería Subterránea*; Informe final. Proyecto 5.3.; LOM: Madrid, Spain, 2015.